Foreground Simulations

V. Jelić and LOFAR-EoR core members

university of groningen
Kapteyn Astronomical Institute

Low Frequency Array - Epoch of Reioization Experiment

Future high redshift 21-cm experiments will suffer from a high degree of contamination, due both to astrophysical foregrounds and to non-astrophysical and instrumental effects. In order to reliably extract the cosmological signal from the observed data, it is essential to understand very well all data components and their influence on the extracted signal. Here we present simulated astrophysical foregrounds data cubes tailored for the LOFAR-EoR experiment and show possible statistical detection of the cosmological 21-cm (EoR) signal.

• Galactic foregrounds

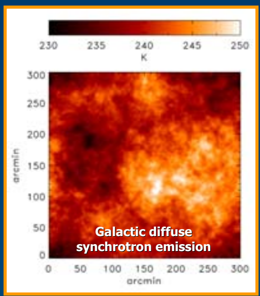

Fig. 1.

@120 MHz

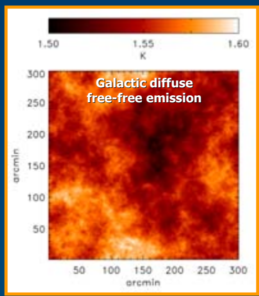

Fig. 2.

Diffuse Galactic synchrotron emission is the dominant component (~ 70%) of the foregrounds and we include all its observed characteristics: spatial and frequency variations of brightness temperature and its spectral index, and brightness temperature variations along the line of sight (*Fig. 1*). Discrete sources of Galactic synchrotron emission are included as observed emission from supernovae remnants.

Despite the minor contribution of the Galactic free-free emission (~ 1%), it is included in our simulations of the foregrounds as an individual component. It has a different temperature spectral index from Galactic synchrotron emission (*Fig. 2*).

• Extragalactic foregrounds

Integrated emission from extragalactic sources is decomposed into two components: emission from radio galaxies and from radio clusters. Simulations of radio galaxies are based on the source count functions at low radio frequency by Jackson (2005), for three different types of radio galaxies, namely FRI, FRII and star forming galaxies. Correlations obtained by radio galaxy surveys are used for their spatial distribution (*Fig. 3*). Simulations of radio clusters are based on a cluster catalogue from the Virgo consortium and observed mass–X-ray luminosity and X-ray–radio luminosity relations (*Fig. 4*).

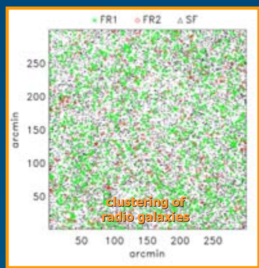

Fig. 3.

@120 MHz

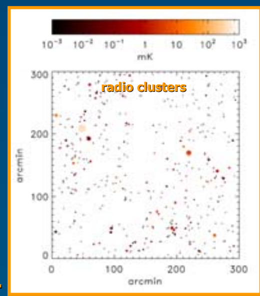

Fig. 4.

• Galactic polarized emission

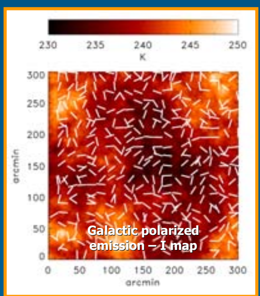

Fig. 5.

@120 MHz

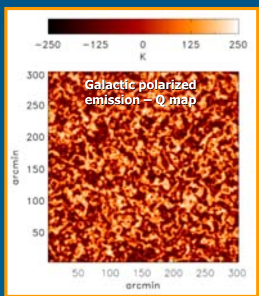

Fig. 6.

In addition to the simulations of the total brightness temperature, the polarized Galactic synchrotron emission maps are produced (*Fig. 5 & 6*). Here, we follow a simple model that includes multiple Faraday screens along the line of sight. The motivation behind these simulations is that improper polarization calibration could severely contaminate the EoR signal, so future robust extraction algorithms have to take this into account.

➢ Statistical detection of the EoR signal

Statistical detection of the EoR signal from the LOFAR-EoR data maps that include diffuse components of the foregrounds and realistic noise (*Fig. 7 & 8*). The solid black line represents the standard deviation (σ) of the noise as a function of frequency, the green dashed line the $\sigma_{residuals}$ after taking out the smooth foreground component ($\sigma^2_{residuals} = \sigma^2_{EoR} + \sigma^2_{noise}$), and the red solid line σ the original EoR signal. The grey shaded zone shows the 2σ detection, whereas the cyan dashed line shows the mean of the detection.

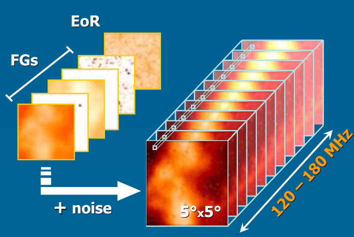

Fig. 7.

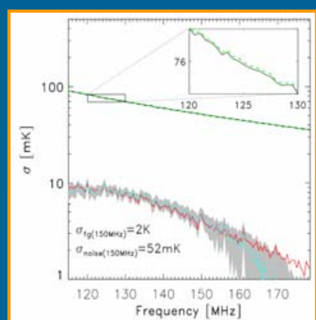

Fig. 8.

We show that with the expected diffuse foreground components and LOFAR-EoR sky and receiver noise levels which amount to 52mK at 150 MHz after 300 hours of total observing time, a simple polynomial fit, along the frequency direction (line by line of sight), allows a statistical reconstruction of the signal.

• **reference:** *Jelic V., et al., 2008, arXiv, 804, arXiv:0804.1130*